
Do Deep Ensembles Actually Capture Uncertainty in Graph Neural Networks?

Pedro C. Vieira^{1,2}

Pedro Ribeiro²

Viacheslav Borovitskiy¹

¹ University of Edinburgh

² DCC/FCUP, University of Porto

Abstract

While deep ensembles are widely considered to be the default method for uncertainty quantification in deep learning, their effectiveness for graph-structured data is often simply assumed based on successes in domains like computer vision. We investigate standard deep ensembles specifically for message-passing graph neural networks. Benchmarking across seven datasets representing varied tasks and complexities, we reveal that ensembles provide surprisingly little improvement over a single model. Instead, the observed marginal gains stem primarily from stabilizing optimization noise in point predictions rather than yielding meaningfully better uncertainty estimates. Through an aleatoric-epistemic decomposition, we identify *epistemic collapse*: independently trained networks consistently converge to overly similar predictions. Because disagreement is the fundamental mechanism through which ensembles capture epistemic uncertainty, this lack of diversity neutralizes their key advantage. Analyzing this phenomenon further, we suggest this collapse is driven by functional rather than weight-space convexity, where distinct parameter solutions induce almost identical behavior. Our results suggest that deep ensemble success does not seamlessly transfer to graph machine learning.

1 Introduction

Uncertainty quantification is essential in high-stakes or automated decision-making applications [18, 37, 56]. Among practical approaches to uncertainty quantification, deep ensembles (DEs) [28] have emerged as a widely used method. Their appeal lies in their simplicity: building a standard deep ensemble requires only the repeated training of a single architecture. Crucially, the disagreement among these independently trained models captures uncertainty that a single model cannot. This mechanism has proven highly effective, establishing deep ensembles as the default for uncertainty quantification in deep learning, provided the added computational cost is not prohibitive [38, 44].

When processing graph-structured data—such as molecules or road networks—uncertainty quantification is much less studied. Here, message-passing neural networks, like graph convolutional (GCN) [25] or attention (GAT) [46] networks, have emerged as one of the dominant architecture classes. While other classes like graph transformers [13, 40] exist, we focus exclusively on message-passing architectures, which we refer to simply as graph neural networks (GNNs) throughout this work. Unlike standard deep learning architectures, GNN computation flow is defined by the structure of the input graph, a property that fundamentally alters the hypothesis space and how optimization trajectories explore it [42, 54]. Naturally, this structural difference can significantly affect how ensembles of such models behave, for better or worse.

At first glance, the literature suggests that DEs are a successful, out-of-the-box solution for uncertainty quantification in graph learning tasks [27, 48]. However, this reputation relies largely on the

Code available at <https://github.com/PedrV/gnn-ug-inspector>.

assumption that the strong uncertainty quantification capabilities of DEs transfer seamlessly from classical deep learning settings like computer vision to graphs. In reality, studies that rigorously scrutinize the uncertainty quality of standard DEs for GNNs are extremely rare.¹ One notable exception is Scalia et al. [43]: focusing exclusively on molecular property prediction with GCNs, they report mixed results. More alarmingly, anecdotal evidence from the PEMS road network benchmark [7, 35] (a graph task explicitly designed to benchmark uncertainty quantification) shows DEs of GNNs failing dramatically and underperforming even a trivial baseline—a failure we revisit in Section 3.

Motivated by these mixed signals, in this paper we aim to provide a sober empirical evaluation of DEs of GNNs. We systematically benchmark these models across multiple tasks, focusing explicitly on the quality of their uncertainty estimates. Our results demonstrate that their behavior in graph settings falls significantly short of expectations inherited from classic deep learning settings, most notably computer vision, where DEs are most widely tested.

A central finding of our study is an empirical phenomenon we term *epistemic collapse*: individual GNNs within a DE exhibit surprisingly limited diversity. Although they are trained independently, their predictions converge to highly similar functions. Because prediction disagreement is the primary mechanism through which deep ensembles capture epistemic uncertainty—the key advantage they offer over a single model—this lack of diversity severely limits their utility. Thus, the ensemble provides little uncertainty improvement over a much cheaper single-model baseline, even though ensemble averaging yields moderate gains in prediction accuracy. Our contributions are:

1. We systematically benchmark standard deep ensembles of GNNs across multiple classic and modern graph machine learning datasets.
2. We empirically demonstrate the phenomenon of epistemic collapse, showing that GNNs tend to converge to highly similar functions regardless of initialization.
3. We demonstrate that the minor improvements in the negative log likelihood (NLL) score provided by DEs are primarily attributable to moderately improved prediction accuracy rather than better uncertainty calibration.
4. We analyze this behavior through the lens of convexity. We hypothesize that the structural properties of GNNs restrict the optimization landscape, driving models toward the same functional solutions and explaining why the success of DEs does not transfer here.

2 Background

Graph neural networks. As mentioned in Section 1, we focus on *message passing graph neural networks* [19]. Let \mathcal{G} be a graph where each node i is associated with a feature vector \mathbf{x}_i . Message passing GNNs build node representations by iteratively exchanging and processing information within local neighborhoods. A typical update at layer ℓ takes the form:

$$\mathbf{h}_i^{(\ell+1)} = \gamma_{\Theta_1} \left(\mathbf{h}_i^{(\ell)}, \bigoplus_{j \in \mathcal{N}(i)} \psi_{\Theta_2} \left(\mathbf{h}_i^{(\ell)}, \mathbf{h}_j^{(\ell)} \right) \right), \quad \mathbf{h}_i^{(0)} = \mathbf{x}_i. \quad (1)$$

Here, $\mathcal{N}(i)$ represents the neighbors of node i , a neural network ψ_{Θ_2} with weights Θ_2 computes messages associated with every neighbor, \bigoplus is a permutation-invariant aggregation function, and γ_{Θ_1} post-processes the aggregated messages. While specific architectures vary—for instance, by incorporating convolution logic as in GCN [25], or attention mechanisms as in GAT [46]—the fundamental inductive bias and computation flow remain tied strictly to the graph topology via (1).

Uncertainty quantification and deep ensembles. Uncertainty quantification aims to measure not just what a model predicts, but how reliable that prediction is. Predictive uncertainty is conceptually divided into *aleatoric* uncertainty, which reflects irreducible noise in the data, and *epistemic* uncertainty, which reflects the model’s lack of knowledge [24].

Originally proposed by Lakshminarayanan et al. [28], deep ensembles (DEs) provide a straightforward, non-Bayesian approach to uncertainty quantification. The method aggregates predictions from

¹Modified ensemble methods exist for specific graph tasks (discussed in Section 2), but here we focus strictly on the standard DE mechanism of repeatedly training the same architecture from different initializations. Because this simple approach is the out-of-the-box standard in classical deep learning, it must serve as the fundamental baseline. However, this fundamental baseline is particularly poorly studied.

M copies of the same architecture trained from different random weight initializations. In a deep ensemble, aleatoric and epistemic uncertainty can be explicitly separated.

For regression, the m -th member of a DE predicts the mean $\mu_m(x)$ and variance $\sigma_m^2(x)$ of a Gaussian distribution. The ensemble prediction is modeled as a Gaussian mixture, yielding an aggregated point prediction $\mu(x) = \frac{1}{M} \sum_{m=1}^M \mu_m(x)$. The total predictive uncertainty is the variance of this mixture, which elegantly decomposes into the average variance and the variance of the means:

$$\underbrace{\sigma^2(x)}_{\text{Total}} = \underbrace{\frac{1}{M} \sum_{m=1}^M \sigma_m^2(x)}_{\text{Aleatoric } \sigma_{\text{ale}}^2(x)} + \underbrace{\frac{1}{M} \sum_{m=1}^M (\mu_m(x) - \mu(x))^2}_{\text{Epistemic } \sigma_{\text{epi}}^2(x)}. \quad (2)$$

For classification, the m -th member of a DE outputs a probability distribution $p_m(y | x)$ over classes. The ensemble outputs a single distribution formed by averaging the member probabilities, $p(y | x) = \frac{1}{M} \sum_{m=1}^M p_m(y | x)$. Here, total uncertainty is measured by the predictive entropy \mathcal{H} , which similarly decomposes into expected data uncertainty and mutual information [11]:

$$\underbrace{\mathcal{H}[p(y | x)]}_{\text{Total}} = \underbrace{\frac{1}{M} \sum_{m=1}^M \mathcal{H}[p_m(y | x)]}_{\text{Aleatoric } \mathcal{H}_{\text{ale}}(x)} + \underbrace{\left(\mathcal{H}[p(y | x)] - \frac{1}{M} \sum_{m=1}^M \mathcal{H}[p_m(y | x)] \right)}_{\text{Epistemic } \mathcal{H}_{\text{epi}}(x)}. \quad (3)$$

2.1 Related Work

Much of the prior work on GNN ensembles diverges from the standard deep ensemble framework by introducing heterogeneous elements. For instance, existing methods ensemble models trained on different graph views [36], employ varied GNN architectures [50], or rely on bootstrapped training data [27]. Other approaches approximate Bayesian inference by sampling from a single optimization trajectory [39] or utilizing stochastic message passing during propagation [29]. In specialized domains like chemistry and material sciences, ensemble methods frequently use highly customized edge-centric architectures, shallow weight sharing, or post-hoc recalibration [10, 23, 45, 47]. Crucially, this heterogeneity confounds the core ensembling mechanism with external inductive biases. If architectural or data diversity is strictly required to generate ensemble disagreement on graphs, it marks a fundamental departure from classical deep learning, where random initialization alone suffices [28, 38]. Because rigorous evaluations of standard, unconfounded deep ensembles on GNNs are rare and paint a conflicting picture [3, 4, 43], we strictly isolate the original ensembling mechanism to systematically evaluate its utility across a broad spectrum of general-purpose graph tasks.

3 A Motivating Example: The PEMS Benchmark

We start by revisiting the PEMS road network benchmark [7]. Originally introduced to evaluate graph Gaussian processes [8], this transductive node regression dataset tasks models with interpolating traffic speeds and quantifying the associated predictive uncertainty.

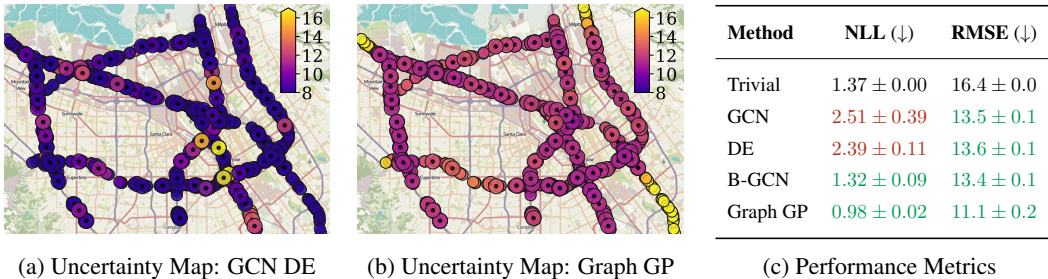


Figure 1: PEMS road network benchmark. Nodes with a black dot in the middle are train nodes. DE produces highly overconfident and uninformative uncertainty estimates (a) compared to the geometrically grounded Graph GP (b). Table (c) confirms that DE fails at uncertainty quantification (NLL), performing significantly worse than Trivial, and only marginally improving over GCN. Red denotes scores worse than trivial and Green better than trivial.

We expand upon the prior evaluation of Borovitskiy [7] by ensuring our base GNNs follow the exact deep ensemble recipe prescribed by Lakshminarayanan et al. [28]. Specifically, we equip the base GCN models with a dedicated variance head to prevent pathologically low aleatoric uncertainty, giving the deep ensemble the best possible chance to succeed. We compare a single GCN, a five-model deep ensemble (DE), a Bayesian GCN (B-GCN) trained via stochastic variational inference [31, 49], and a Matérn Gaussian process on the graph (Graph GP) [8]. As a sanity check, we include a *Trivial* baseline that predicts a constant Gaussian distribution $N(\mu_{\text{train}}, \sigma_{\text{train}}^2)$ derived directly from the training labels. For more details on the setup, see Appendix A.

The results, shown in Figure 1, reveal a striking failure of the deep ensemble. While it improves point estimation (RMSE) over the Trivial baseline, its uncertainty quantification is catastrophically poor, yielding a significantly worse NLL score. Visually (Figures 1a and 1b), the Graph GP produces a dynamic uncertainty map that sensibly increases away from training data. In stark contrast, the GCN DE produces a pathologically low, uninformative confidence landscape that sometimes spontaneously spikes at training nodes. Crucially, the Bayesian GCN utilizes the exact same architecture yet achieves an NLL that comfortably beats the Trivial baseline. This suggests that the failure stems not from a lack of expressivity in the GNN architecture itself, but rather from the interplay between message passing and the deep ensemble mechanism. Finally, the Graph GP achieves the best overall performance; this is theoretically expected because the absence of rich node features on this dataset strips GNNs of their primary informational advantage, making the task hard for them.

This motivating example raises a critical question: *Is the failure on PEMS an isolated anomaly, or is it symptomatic of a broader incompatibility between deep ensembles and graph neural networks?*

4 Benchmarking Ensembles of Graph Neural Networks

While the PEMS benchmark provides anecdotal evidence of deep ensembles failing on GNNs, we must establish whether this is an isolated anomaly or a systemic issue. To answer this, we conduct a comprehensive evaluation of GNN ensembles across a diverse suite of graph machine learning tasks.

Datasets. In total, we evaluate on seven diverse graph datasets spanning node classification, node regression, and graph regression. Having established the catastrophic failure on the PEMS (PEMS) road network in Section 3, we focus here on the remaining six datasets. For node classification, we include the classic Cora (CORA) and Citeseer (CTSR) benchmarks [55]. To address the limitations of these older, smaller datasets, we add Tolokers2 (TLK2) [5]. For node regression, we use Artnetviews (ARTNV) [5] and Chameleon (CHAM) [41], which offer larger, structurally challenging, and more realistic evaluation settings. CHAM exhibits benign heterophily [33], providing a fundamentally different neighborhood structure while remaining suitable for GNNs. Finally, for graph-level regression, we use the classic QM9 dataset [53]. We subsample QM9 to 5% of its original size (denoted QM9-5%) and restrict to the HOMO-LUMO gap prediction task, one of the most difficult in the dataset. We stratify this subsampling by the target variable to preserve its overall distribution. We deliberately

Table 1: Absolute performance metrics for a DE of five models. Values represent NLL, ECE (for regression stands for miscalibration area), and point estimation metric (PEM: RMSE for regression and accuracy for classification), showing the mean and standard deviation over 10 independent runs. The ECE of the trivial baseline is not taken into account when highlighting the best score. Low ECE for the trivial baseline is theoretically expected.

		Classification			Regression		
		CORA	CTSR	TLK2	ARTNV	CHAM	QM9-5%
Trivial	NLL	1.940 ± 0.000	1.792 ± 0.000	0.525 ± 0.000	1.425 ± 0.000	1.415 ± 0.000	1.404 ± 0.000
	ECE	0.116 ± 0.000	0.069 ± 0.000	0.000 ± 0.000	0.015 ± 0.000	0.072 ± 0.000	0.070 ± 0.000
	PEM	0.130 ± 0.000	0.077 ± 0.000	0.782 ± 0.000	1.715 ± 0.000	2.160 ± 0.000	1.268 ± 0.000
GNN	NLL	0.612 ± 0.009	0.929 ± 0.003	0.371 ± 0.002	0.993 ± 0.005	0.868 ± 0.066	0.833 ± 0.021
	ECE	0.123 ± 0.001	0.142 ± 0.002	0.079 ± 0.000	0.033 ± 0.017	0.137 ± 0.054	0.568 ± 0.014
	PEM	0.806 ± 0.006	0.710 ± 0.004	0.854 ± 0.005	1.113 ± 0.006	1.215 ± 0.044	0.384 ± 0.014
DE	NLL	0.600 ± 0.008	0.929 ± 0.001	0.367 ± 0.001	0.958 ± 0.004	0.749 ± 0.026	0.803 ± 0.003
	ECE	0.122 ± 0.002	0.141 ± 0.002	0.077 ± 0.005	0.009 ± 0.002	0.266 ± 0.027	0.595 ± 0.004
	PEM	0.808 ± 0.003	0.711 ± 0.000	0.856 ± 0.002	1.086 ± 0.004	1.132 ± 0.022	0.362 ± 0.005

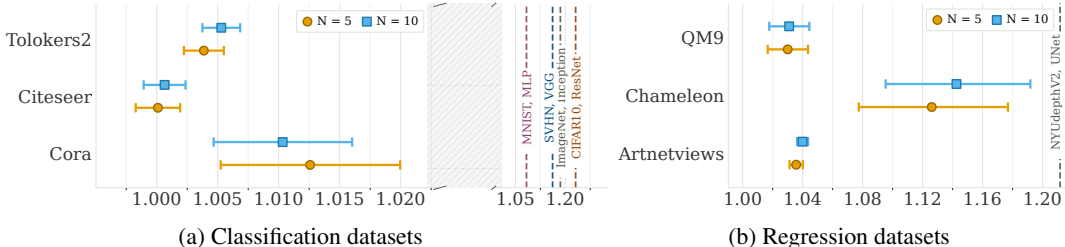


Figure 2: Likelihood ratios $\exp(\text{NLL}_{\text{GNN}} - \text{NLL}_{\text{DE}})$ and 95% Gaussian confidence intervals. This quantifies the relative predictive likelihood improvement of DE over GNN for both classification and regression datasets. Baselines indicate typical improvements observed in foundational DE literature.

implement this subsampling to test a data-scarce regime, a setting where the quality of uncertainty estimates is especially critical. Together, these datasets capture diverse graph learning settings.

Models. We select architectures that represent standard practice for each task. For CORA, CTSR, ARTNV, and QM9-5%, we employ standard GCNs [25]. On ARTNV, the GCN is the established state-of-the-art [5]. While attention-based models can yield marginal improvements on CORA and CTSR, GCNs are often preferred for their superior training stability and simplicity, hence our choice. For QM9-5%, although top-performing methods utilize 3D spatial coordinates, GCNs perform comparably to other purely topological GNNs [17, 53] and provide a clean, representative baseline. Conversely, we utilize GATv2 architectures [9] for CHAM and TLK2, where empirical evidence strongly favors attention mechanisms. Specifically, GATv2 constitutes the known state-of-the-art for TLK2 [5]. For regression tasks, we equip each architecture with an additional variance head to capture aleatoric uncertainty, jointly optimizing the predictive mean and variance by maximizing the likelihood. All models are optimized to achieve performance levels commensurate with the established literature. Full architectural and hyperparameter configurations are deferred to Appendix A.

Metrics. Our primary metric for jointly evaluating predictive performance and uncertainty quality is the negative log-likelihood (NLL) score. For finer-grained insights, we evaluate separate metrics that isolate predictive accuracy from uncertainty calibration. Specifically, we report the root mean squared error (RMSE) for regression and accuracy for classification. To assess calibration, we compute the expected calibration error (ECE) [22] for classification and the analogous expected coverage error (ECE; termed *miscalibration area* in Tran et al. [44]) for regression. We report the mean and standard deviation of these metrics across ten independent runs.

Results. In contrast to the pathological failure on PEMS, Table 1 shows that deep ensembles generally outperform the Trivial baseline across all other datasets. They improve both point estimation and NLL compared to a single GNN in most cases, though the resulting gains appear modest and calibration (ECE) sometimes distinctly degrades, as seen on CHAM and QM9-5%. To properly analyze this behavior, we must ask: how do these improvements actually compare to the established literature?

To answer this question and quantify the performance gap, we compute the likelihood ratios: $\exp(\text{NLL}_{\text{GNN}} - \text{NLL}_{\text{DE}})$. They provide an interpretable measure of the relative gain of an ensemble over a single model, representing the multiplicative factor by which the ensemble increases the likelihood of the test labels.² Figure 2 compares these ratios against historical improvements derived from foundational deep ensemble literature predominantly anchored in computer vision [28, 30, 34].

For classification tasks, the contrast is drastic: while classic computer vision benchmarks report ensembles assigning roughly 20% more likelihood to test points than a single model, our graph ensembles yield improvements ranging from merely 0.1% to 1%. In regression, the reference computer vision baseline similarly shows a $\sim 20\%$ improvement, whereas our graph ensembles typically assign only about 5% more likelihood to the test data. Even the most favorable case, CHAM, peaks at

²We avoid reporting relative percentage changes in NLL. Since log-likelihood lacks an absolute zero and can be negative, especially in continuous settings, direct ratios are mathematically flawed. We instead report the exponentiated difference, providing a sound and intuitive likelihood ratio.

roughly 14% improvement, which is not only well below the standard computer vision baseline but also exhibits a wide confidence interval, meaning the gains of a DE are highly unstable.

Crucially, Table 1 reveals that improvements in NLL are consistently coupled with improvements in accuracy or RMSE. Because NLL is a composite metric, these likelihood gains might be driven entirely by slightly more accurate point estimates rather than genuinely improved uncertainty calibration. To determine whether deep ensembles on graphs actually fulfill their primary purpose—improving uncertainty quantification—we must further analyze these mechanisms in isolation.

Larger ensembles and distribution shift. While we report results for ensembles of five models here, we attest that these limitations are persistent. As detailed in Appendix C, scaling the ensembles to ten models yields virtually identical trends. Additionally, evaluating deep ensembles under covariate shift on purpose-built splits for ARTNV and TLK2 reveals that the relative improvements over a single GNN remain just as marginal, if not worse, than in the in-distribution setting (Appendix B).

5 Disentangling Performance: Do Deep Ensembles Improve Uncertainty?

While Section 4 shows that deep ensembles somewhat reduce NLL, we must disentangle whether these gains reflect genuinely better uncertainty quantification or merely more accurate point predictions. To this end, in Section 5.1, we deconstruct the improvements of deep ensembles, revealing that the modest gains in NLL are driven almost entirely by variance reduction and predictive accuracy rather than better uncertainty estimates. Further, in Section 5.2, we investigate *why* this occurs by analyzing ensemble diversity. We identify a systemic phenomenon we term *epistemic collapse*, wherein individual GNNs in an ensemble fail to explore diverse functional hypotheses.

5.1 Deconstructing the NLL Gains

Because regression and classification parameterize uncertainty differently, we require distinct methodologies to trace the source of the NLL improvements. For regression, we can explicitly decouple the predicted mean from the predicted variance to isolate point prediction gains. For classification, where point estimates and uncertainty are inherently entangled in the predicted probability distribution, we instead analyze the distributional benefit of ensembling via Jensen’s inequality gap.

Regression. To isolate the contribution of the ensemble’s point prediction, we evaluate two constructed baselines alongside a standard single GNN and a full DE. The first baseline pairs the DE’s mean prediction—the average of the individual means—with the variance of a randomly selected single model (DE-R). The second baseline pairs the DE’s mean prediction with only the aleatoric variance (DE-A), which is the average of the individual variances (cf. Equation (2)).

Figure 3a displays the NLL performance for the GNN, DE, DE-R, and DE-A models. Notably, all models utilizing the DE mean (DE, DE-R, DE-A) achieve nearly identical NLL improvements over the single-model baseline. Thus, the already modest NLL gains are driven almost exclusively by the ensembled mean providing a smoothed, slightly more accurate point prediction, rather than the ensemble supplying a better-calibrated measure of uncertainty. This directly explains the paradox observed in Table 1, where DEs improve NLL on datasets like CHAM and QM9-5% while simultaneously worsening the calibration error (ECE). Furthermore, the distribution of NLL scores in Figure 3a reveals another key insight. We observe that the best-performing single models can sometimes reach NLL scores comparable to those of the full ensemble or get extremely close.³ This suggests that ensembling in this context acts primarily as a variance reduction technique over optimization noise, stabilizing the performance of a single model rather than fundamentally improving it.

Classification. Unlike regression, classification inherently entangles point estimates and confidence scores within a single predicted probability distribution. To understand if the ensemble genuinely improves this distribution—for instance, by tempering overconfident predictions—we analyze the gap between the expected NLL of an individual model and the NLL of the ensemble. Let $p_m(y | x)$ be the probability assigned to the true class y by the m -th model. Because the negative logarithm is strictly convex, Jensen’s inequality ensures the ensemble’s NLL is bounded by the average individual

³Because the data splits are fixed across all runs, the variance stems entirely from the random initialization.

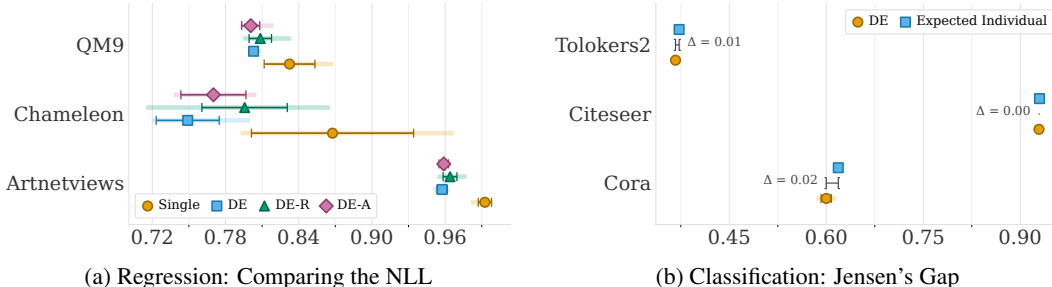


Figure 3: Deconstructing the source of NLL improvements. (a) compares the NLL of a GNN, a DE, and two additional baselines (DE-R and DE-A) that isolate the point prediction improvement effect. (b) visualizes the nonnegative gap between the expected individual NLL and the ensemble’s NLL (Jensen’s gap). The marker represents mean, thin bars represent $\pm\sigma$ and transparent ones min–max.

NLL:

$$\underbrace{-\log\left(\frac{1}{M}\sum_{m=1}^M p_m(y|x)\right)}_{\text{NLL}_{\text{DE}}} \leq \underbrace{\frac{1}{M}\sum_{m=1}^M -\log p_m(y|x)}_{\text{Expected Individual NLL}}. \quad (4)$$

The difference between the RHS and LHS (Jensen’s gap) isolates the NLL reduction derived from genuine improvements in the predictive distribution, filtering out gains from mere stabilization.

As shown in Figure 3b, this gap is remarkably small across all tested graph classification datasets. This near-zero gap implies that the individual models are outputting practically identical probability distributions. Because the ensembled distributions are virtually indistinguishable from the individual ones, the ensemble provides no fundamental enhancement to the predictive capabilities of the model. Instead, just as in the regression setting, we observe that ensembling acts as a variance reduction mechanism over optimization noise. The variance in performance across random initializations heavily dominates the actual ensembling effect, meaning the best-performing individual models in our runs sometimes nearly match or even improve the NLL of the full ensemble.

5.2 Diversity and Epistemic Collapse

In Section 5.1, we established that DEs of GNNs act primarily as variance-reducing smoothers. To understand why this happens, we must consider the fundamental mechanism deep ensembles use to quantify uncertainty: the disagreement among their constituent models [1, 12, 28]. This disagreement determines the epistemic component of uncertainty (Equations (2) and (3))—the primary contribution of a deep ensemble to uncertainty quantification over a single model. If the individual GNNs fail to meaningfully disagree, the ensemble cannot capture epistemic uncertainty and naturally reduces to a mere smoother. To confirm that this mechanism explains our earlier evidence, we investigate whether GNN ensembles suffer from a phenomenon we term *epistemic collapse*: a systemic failure of independently trained models to explore diverse functional hypotheses.

To verify this, Figure 4 displays the breakdown of predictive uncertainty into its aleatoric and epistemic parts. The results are remarkably consistent across tasks: the predictive uncertainty of GNN ensembles is overwhelmingly aleatoric-dominant. In regression, the epistemic variance is consistently dwarfed by the aleatoric variance. In classification, after normalizing by the maximum entropy $\log C$, the epistemic entropy is close to zero, with maxima rarely exceeding 0.1. This empirically confirms the presence of epistemic collapse: despite independent random initializations, the models converge to very similar predictions, leaving the epistemic component too weak to be useful.

This behavior deviates sharply from expectations established in classic deep learning settings. For instance, Kendall and Gal [24] report an epistemic-to-aleatoric ratio of roughly 5 for in-distribution regression in computer vision. In contrast, our graph regression models frequently exhibit ratios well below 1. For classification, while recent literature reports isolated instances of epistemic collapse, it typically occurs only in highly over-parameterized models or massive ensembles [15, 26]. We observe significantly smaller values than prior work using similar normalization procedures, a discrepancy that persists across standard architectures and datasets of varying structures. Our re-

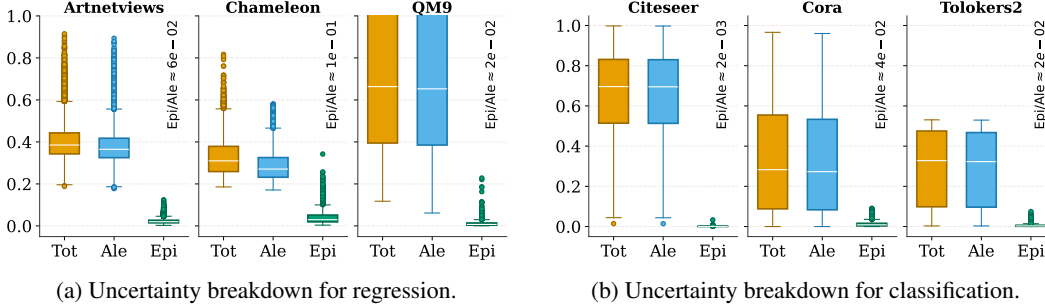


Figure 4: Comparison of epistemic, aleatoric, and total uncertainty across datasets, demonstrating the *epistemic collapse*. For both regression and classification, the epistemic part of uncertainty collapses to near-zero values, while aleatoric uncertainty remains relatively large.

sults demonstrate that for GNNs, this collapse is not an edge case but a severe, systemic feature. Ultimately, because individual GNNs converge to highly similar functions, they neutralize the exact mechanism deep ensembles rely on to improve uncertainty quantification.

6 Discussion: GNNs and Convexity

Fundamentally, deep ensembles are expected to disagree because they explore a complex, highly non-convex, and multi-modal loss landscape [16]. If independently trained models consistently converge to the same solution, it suggests that the optimization landscape they traverse behaves more like a convex optimization problem, where all paths lead toward the same basin. Given the widespread epistemic collapse we observe, we hypothesize that GNNs operate in a regime that induces this convex-like behavior. Because the exact theoretical cause remains unproven, we frame this section as a discussion of potential mechanisms and an open problem for future research.

This hypothesis finds an interesting parallel in computer vision. Ovadia et al. [38] observe that on MNIST, deep ensembles lose their typical advantage over mode-seeking variational inference, whereas they strongly dominate on complex image datasets. We speculate that the simplicity of the MNIST task coupled with the used model architectures might induce a smoother, more convex-like optimization landscape, naturally limiting the functional diversity of an ensemble. In our graph experiments, however, we observe epistemic collapse across a wide array of benchmarks of varying complexity. This strongly suggests that for GNNs, this convex-like behavior is not a byproduct of the dataset, but rather a product of the message-passing architecture itself.

Furthermore, this hypothesis aligns with a well-known phenomenon in graph learning. Wu et al. [52] introduced *Simplified Graph Convolutions (SGC)*, demonstrating that on certain tasks, standard GCNs can be stripped of their intermediate non-linearities and collapsed into a fixed low-pass graph filter followed by a linear transformation. While expressive GNNs remain necessary for modeling highly complex non-linear graph dependencies, the fact that such a dramatic linear simplification can often maintain competitive performance is indicative. It implies that, despite the depth of standard GNNs, their underlying optimization landscape may in fact be remarkably simple and behave much like that of a convex linear problem.

When deep learning models exhibit this kind of convex-like simplicity, it can manifest in two distinct ways: in the weight space, or in the functional space. Convexity in the weight space means the loss landscape itself forms a simple basin, causing independent training runs to converge to the exact same neighborhood of weights. Convexity in the functional space, on the other hand, implies that while the models might converge to completely different regions of a highly non-convex weight landscape, those distinct weight configurations all implement the same (or similar) function.

To distinguish which of these two regimes governs GNNs, we test the convexity in the weight space. To this end, we construct a “model soup” [51] by averaging the weights of the individual ensemble members. If the models resided within a simple convex basin in the weight space, averaging their weights would act as a variance reduction mechanism over a noisy approximation of the global optimum, yielding a point closer to the true global optimum and thus improving performance. However,

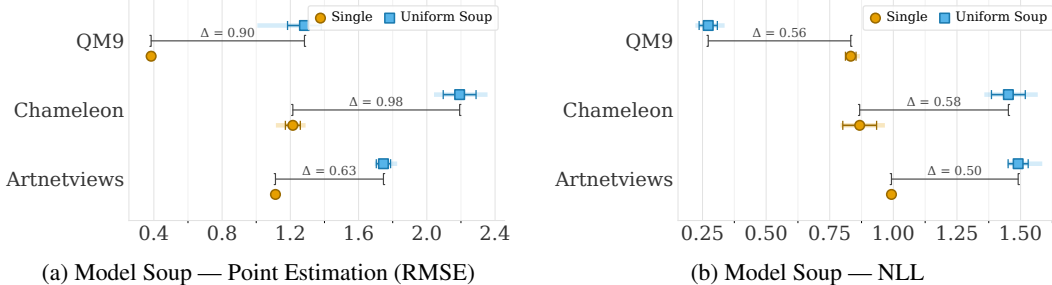


Figure 5: Weight-space convexity analysis. (a) compares the point prediction performance and (b) compares the NLL of a single model against a model soup formed by averaging the weights of the ensemble members. The degraded performance of the model soup confirms that the models reside in different regions of a highly non-convex weight space. Markers represent the mean, thin bars represent $\pm\sigma$ and transparent bars represent min–max.

as shown in Figure 5, the model soup generally underperforms a single model (Appendix C shows a similar analysis for classification). For point prediction, its performance degrades to essentially match a Trivial baseline. In the only case where the aggregate NLL metric technically improves (QM9–5%), the soup remains practically uninformative for uncertainty quantification, as it outputs near-identical uncertainties for all predictions. This degraded behavior confirms that the weight space itself remains highly non-convex—a natural consequence once one considers the permutation symmetries inherent in deep neural networks [2, 14].

Therefore, we are left with a compelling hypothesis: the weight space is non-convex, yet epistemic collapse strongly suggests that GNNs experience a form of convexity in the *functional* space. That is, independently trained models find different sets of weights that ultimately implement the same (or similar) predictive function. This functional collapse might be conceptually connected to the well-documented phenomenon of oversmoothing, where node representations become indistinguishable after repeated message-passing steps. However, because we utilize optimally tuned, shallow layer depths, our models should not suffer from classical oversmoothing. Instead, this suggests that the homogenizing effect of message passing might act as a more fundamental architectural bias that restricts functional diversity even in shallow networks. We leave the precise theoretical explanation of how message passing causes this functional convexity as an open problem—one that promises to improve our fundamental understanding of GNNs for uncertainty quantification and beyond.

7 Conclusion

We can now directly answer the research question posed in Section 3. While the catastrophic failure on the PEMS benchmark—performing worse than a Trivial baseline—is an anomaly, our evaluation confirms it is symptomatic of a broader underlying issue. This leads us to the overarching question of the paper’s title: *Do deep ensembles actually capture uncertainty in graph neural networks?* Our results demonstrate that they largely do not—at least, not beyond what a single constituent model already captures. Although deep ensembles of GNNs typically outperform the Trivial baseline, they consistently fail to deliver meaningful improvements in uncertainty quantification. Unlike in classic computer vision settings, where ensembles have been shown to capture critical epistemic uncertainty, GNN ensembles suffer from epistemic collapse. Their minor NLL improvements stem almost entirely from the variance-reducing smoothing effect of better point predictions through averaging.

Practically, this renders the standard deep ensemble recipe inefficient for message-passing graph neural networks. Training and deploying an ensemble incurs a multiplicative computational and memory cost. Yet, because the models lack functional diversity, the ensemble merely stabilizes optimization noise. Consequently, a single “lucky” model—selected simply by choosing the best-performing random initialization on a validation set—can often match or even exceed the NLL performance of the full ensemble. While finding this optimal seed still requires the upfront computational cost of training multiple models, deploying only the single best network drastically reduces compute and memory overhead during inference. Ultimately, high-quality uncertainty quantification in graph learning requires moving beyond naive ensembling of message-passing architectures.

Acknowledgements

Pedro C. Vieira and Pedro Ribeiro are funded by national funds through FCT – Fundação para a Ciência e a Tecnologia, I.P., under the PhD scholarship 2025.02316.BD and under the grant UID/50014/2025.

References

- [1] T. Abe, E. K. Buchanan, G. Pleiss, R. Zemel, and J. P. Cunningham. Deep ensembles work, but are they necessary? In *Advances in Neural Information Processing Systems*, 2022. Cited on page 7.
- [2] S. Ainsworth, J. Hayase, and S. Srinivasa. Git Re-Basin: Merging Models modulo Permutation Symmetries. In *International Conference on Learning Representations*, 2023. Cited on page 9.
- [3] G. Bazhenov, S. Ivanov, M. Panov, A. Zaytsev, and E. Burnaev. Towards OOD Detection in Graph Classification from Uncertainty Estimation Perspective. *arXiv preprint arXiv:2206.10691*, 2022. Cited on page 3.
- [4] G. Bazhenov, D. Kuznedelev, A. Malinin, A. Babenko, and L. Prokhorenkova. Evaluating Robustness and Uncertainty of Graph Models Under Structural Distributional Shifts. In *Advances in Neural Information Processing Systems*, 2023. Cited on pages 3, 13.
- [5] G. Bazhenov, O. Platonov, and L. Prokhorenkova. GraphLand: Evaluating Graph Machine Learning Models on Diverse Industrial Data. In *The Thirty-ninth Annual Conference on Neural Information Processing Systems Datasets and Benchmarks Track*, 2025. Cited on pages 4, 5, 14, 15.
- [6] C. Blundell, J. Cornebise, K. Kavukcuoglu, and D. Wierstra. Weight uncertainty in neural networks. In *International Conference on International Conference on Machine Learning*, 2015. Cited on page 13.
- [7] V. Borovitskiy. PeMS Regression: A Benchmark Suite for Node Regression with Uncertainty, 2025. URL: <https://github.com/vabor112/pems-regression>. Cited on pages 2–4, 13.
- [8] V. Borovitskiy, I. Azangulov, A. Terenin, P. Mostowsky, M. Deisenroth, and N. Durrande. Matérn Gaussian processes on graphs. In *International Conference on Artificial Intelligence and Statistics*, 2021. Cited on pages 3, 4.
- [9] S. Brody, U. Alon, and E. Yahav. How Attentive are Graph Attention Networks? In *International Conference on Learning Representations*, 2022. Cited on page 5.
- [10] J. Busk, P. Bjørn Jørgensen, A. Bhowmik, M. N. Schmidt, O. Winther, and T. Vegge. Calibrated uncertainty for molecular property prediction using ensembles of message passing neural networks. *Machine Learning: Science and Technology*, 3, 2021. Cited on page 3.
- [11] S. Depeweg, J.-M. Hernandez-Lobato, F. Doshi-Velez, and S. Udluft. Decomposition of Uncertainty in Bayesian Deep Learning for Efficient and Risk-sensitive Learning. In *International Conference on Machine Learning*, 2018. Cited on page 3.
- [12] T. G. Dietterich. Ensemble Methods in Machine Learning. In *Multiple Classifier Systems*, 2000. Cited on page 7.
- [13] V. P. Dwivedi and X. Bresson. A generalization of transformer networks to graphs. *arXiv preprint arXiv:2012.09699*, 2020. Cited on page 1.
- [14] R. Entezari, H. Sedghi, O. Saukh, and B. Neyshabur. The Role of Permutation Invariance in Linear Mode Connectivity of Neural Networks. In *International Conference on Learning Representations*, 2022. Cited on page 9.
- [15] M. Fellaji and F. Pennerath. The Epistemic Uncertainty Hole: an issue of Bayesian Neural Networks, 2024. Cited on page 7.
- [16] S. Fort, H. Hu, and B. Lakshminarayanan. Deep Ensembles: A Loss Landscape Perspective. *arXiv preprint arXiv:1912.02757*, 2019. Cited on page 8.
- [17] V. Fung, J. Zhang, E. Juarez, and B. G. Sumpter. Benchmarking graph neural networks for materials chemistry. *npj Computational Materials*, 7(1):84, 2021. Cited on page 5.
- [18] R. Garnett. *Bayesian optimization*. Cambridge University Press, 2023. Cited on page 1.

- [19] J. Gilmer, S. S. Schoenholz, P. F. Riley, O. Vinyals, and G. E. Dahl. Neural message passing for Quantum chemistry. In *International Conference on Machine Learning*, 2017. Cited on page 2.
- [20] X. Glorot and Y. Bengio. Understanding the difficulty of training deep feedforward neural networks. In *International Conference on Artificial Intelligence and Statistics*, 2010. Cited on page 13.
- [21] A. Graves. Practical Variational Inference for Neural Networks. In *Advances in Neural Information Processing Systems*, 2011. Cited on page 13.
- [22] C. Guo, G. Pleiss, Y. Sun, and K. Q. Weinberger. On calibration of modern neural networks. In *International Conference on Machine Learning*, 2017. Cited on page 5.
- [23] L. Hirschfeld, K. Swanson, K. Yang, R. Barzilay, and C. W. Coley. Uncertainty Quantification Using Neural Networks for Molecular Property Prediction. *Journal of Chemical Information and Modeling*, 60, 2020. Cited on page 3.
- [24] A. Kendall and Y. Gal. What uncertainties do we need in Bayesian deep learning for computer vision? In *Advances in Neural Information Processing Systems*, 2017. Cited on pages 2, 7.
- [25] T. N. Kipf and M. Welling. Semi-Supervised Classification with Graph Convolutional Networks. In *International Conference on Learning Representations*, 2017. Cited on pages 1, 2, 5.
- [26] A. Kirsch. (Implicit) Ensembles of Ensembles: Epistemic Uncertainty Collapse in Large Models. *Transactions on Machine Learning Research*, 2025. Cited on page 7.
- [27] S. Krieg, W. Burgis, P. Soga, and N. Chawla. Deep Ensembles for Graphs with Higher-order Dependencies. In *International Conference on Learning Representations*, 2023. Cited on pages 1, 3.
- [28] B. Lakshminarayanan, A. Pritzel, and C. Blundell. Simple and Scalable Predictive Uncertainty Estimation using Deep Ensembles. In *Advances in Neural Information Processing Systems*, 2017. Cited on pages 1–5, 7.
- [29] Q. Lin, S. Yu, K. Sun, W. Zhao, O. Alfarraj, A. Tolba, and F. Xia. Robust Graph Neural Networks via Ensemble Learning. *Mathematics*, 10, 2022. Cited on page 3.
- [30] J. Z. Liu, Z. Lin, S. Padhy, D. Tran, T. Bedrax-Weiss, and B. Lakshminarayanan. Simple and principled uncertainty estimation with deterministic deep learning via distance awareness. In *Advances in Neural Information Processing Systems*, 2020. Cited on page 5.
- [31] C. Louizos and M. Welling. Multiplicative normalizing flows for variational Bayesian neural networks. In *International Conference on Machine Learning*, 2017. Cited on pages 4, 13.
- [32] C. Louizos and M. Welling. Structured and efficient variational deep learning with matrix Gaussian posteriors. In *International Conference on International Conference on Machine Learning*, 2016. Cited on page 13.
- [33] S. Luan, Q. Lu, C. Hua, X. Wang, J. Zhu, and X.-W. Chang. Re-evaluating the Advancements of Heterophilic Graph Learning. *arXiv preprint arXiv:2409.05755*, 2024. Cited on page 4.
- [34] H. Manh Bui and A. Liu. Density-Regression: Efficient and Distance-aware Deep Regressor for Uncertainty Estimation under Distribution Shifts. In *International Conference on Artificial Intelligence and Statistics*, 2024. Cited on page 5.
- [35] P. Mostowsky, V. Dutordoir, I. Azangulov, N. Jaquier, M. J. Hutchinson, A. Ravuri, L. Rozo, A. Terenin, and V. Borovitskiy. The GeometricKernels Package: Heat and Matérn Kernels for Geometric Learning on Manifolds, Meshes, and Graphs. *Journal of Machine Learning Research*, 2025. Cited on page 2.
- [36] V. T. Nguyen, D. A. Pham, A. T. Le, J. Peter, and G. Gust. Persistent Homology-induced Graph Ensembles for Time Series Regressions. *arXiv preprint arXiv:2503.14240*, 2025. Cited on page 3.
- [37] J. Ojha, O. Presacan, P. G. Lind, E. Monteiro, and A. Yazidi. Navigating Uncertainty: A User-Perspective Survey of Trustworthiness of AI in Healthcare. *ACM Trans. Comput. Healthcare*, 6, 2025. Cited on page 1.
- [38] Y. Ovadia, E. Fertig, J. Ren, Z. Nado, D. Sculley, S. Nowozin, J. Dillon, B. Lakshminarayanan, and J. Snoek. Can you trust your model’s uncertainty? Evaluating predictive uncertainty under dataset shift. In *Advances in Neural Information Processing Systems*, 2019. Cited on pages 1, 3, 8, 13.

- [39] C. M. A. Rahman, G. Bhandari, N. M. Nasrabadi, A. H. Romero, and P. K. Gyawali. Enhancing material property prediction with ensemble deep graph convolutional networks. *Frontiers in Materials*, 11, 2024. Cited on page 3.
- [40] L. Rampásek, M. Galkin, V. P. Dwivedi, A. T. Luu, G. Wolf, and D. Beaini. Recipe for a general, powerful, scalable graph transformer. In *Advances in Neural Information Processing Systems*, 2022. Cited on page 1.
- [41] B. Rozemberczki, C. Allen, and R. Sarkar. Multi-Scale attributed node embedding. *Journal of Complex Networks*, 9, 2021. Cited on page 4.
- [42] T. K. Rusch, M. M. Bronstein, and S. Mishra. A survey on oversmoothing in graph neural networks. *arXiv preprint arXiv:2303.10993*, 2023. Cited on page 1.
- [43] G. Scalia, C. A. Grambow, B. Pernici, Y.-P. Li, and W. H. Green. Evaluating Scalable Uncertainty Estimation Methods for Deep Learning-Based Molecular Property Prediction. *Journal of Chemical Information and Modeling*, 60, 2020. Cited on pages 2, 3.
- [44] K. Tran, W. Neiswanger, J. Yoon, Q. Zhang, E. Xing, and Z. W. Ulissi. Methods for comparing uncertainty quantifications for material property predictions. *Machine Learning: Science and Technology*, 1, 2020. Cited on pages 1, 5.
- [45] D. Varivoda, R. Dong, S. S. Omee, and J. Hu. Materials Property Prediction with Uncertainty Quantification: A Benchmark Study. *arXiv preprint arXiv:2211.02235*, 2022. Cited on page 3.
- [46] P. Veličković, G. Cucurull, A. Casanova, A. Romero, P. Liò, and Y. Bengio. Graph Attention Networks. In *International Conference on Learning Representations*, 2018. Cited on pages 1, 2.
- [47] T. Vinchurkar, K. Abdelmaqsoud, and J. R. Kitchin. Uncertainty quantification in graph neural networks with shallow ensembles. *Machine Learning: Science and Technology*, 6, 2025. Cited on page 3.
- [48] F. Wang, Y. Liu, K. Liu, Y. Wang, S. Medya, and P. S. Yu. Uncertainty in Graph Neural Networks: A Survey. *Transactions on Machine Learning Research*, 2024. Cited on page 1.
- [49] Y. Wen, P. Vicol, J. Ba, D. Tran, and R. Grosse. Flipout: Efficient Pseudo-Independent Weight Perturbations on Mini-Batches. *arXiv preprint arXiv:1803.04386*, 2018. Cited on pages 4, 13.
- [50] Z. H. Wong, L. Yue, and Q. Yao. Ensemble Learning for Graph Neural Networks. *arXiv preprint arXiv:2310.14166*, 2023. Cited on page 3.
- [51] M. Wortsman, G. Ilharco, S. Y. Gadre, R. Roelofs, R. Gontijo-Lopes, A. S. Morcos, H. Namkoong, A. Farhadi, Y. Carmon, S. Kornblith, and L. Schmidt. Model soups: averaging weights of multiple fine-tuned models improves accuracy without increasing inference time. In *International Conference on Machine Learning*, 2022. Cited on pages 8, 14.
- [52] F. Wu, A. Souza, T. Zhang, C. Fifty, T. Yu, and K. Weinberger. Simplifying Graph Convolutional Networks. In *International Conference on Machine Learning*, 2019. Cited on page 8.
- [53] Z. Wu, B. Ramsundar, E. N. Feinberg, J. Gomes, C. Geniesse, A. S. Pappu, K. Leswing, and V. Pande. MoleculeNet: a benchmark for molecular machine learning. *Chemical Science*, 9, 2018. Cited on pages 4, 5.
- [54] K. Xu, W. Hu, J. Leskovec, and S. Jegelka. How Powerful are Graph Neural Networks? In *International Conference on Learning Representations*, 2019. Cited on page 1.
- [55] Z. Yang, W. W. Cohen, and R. Salakhutdinov. Revisiting semi-supervised learning with graph embeddings. In *International Conference on International Conference on Machine Learning*, 2016. Cited on page 4.
- [56] Q. Zhu, W. Li, H. Kim, Y. Xiang, K. Wardega, Z. Wang, Y. Wang, H. Liang, C. Huang, J. Fan, and H. Choi. Know the unknowns: addressing disturbances and uncertainties in autonomous systems. In *International Conference on Computer-Aided Design*, 2020. Cited on page 1.

A Extra Details on the Experiments Conducted

Like in the main text each experiment is repeated ten times to obtain the required statistics. Furthermore, for all plots in these sections, the marker indicates the mean improvement. The thick whisker denotes $\pm\sigma$, and the thin semi-transparent lines represent the minimum and maximum values.

The selected hyperparameters used throughout the experiments in the main text are displayed in Table 2. For the GAT models, the number of attention heads used was four. For Tolokers2, Artnetviews and Chameleon, besides the GNN we used a multi-layer perceptron (MLP) module to pre-process the input. We also apply an MLP in between the GNN layers and after the output of the final GNN layer. The MLP used has depth two. The model for QM9 also includes a pooling mechanism to create the graph level representations. This mechanism concatenates the representations obtained from the basic pooling mechanisms: mean, maximum and standard deviation. This representation is then used as input for a two layer MLP with 256 hidden dimension that will produce the final graph level representation.

Table 2: Hyperparameter configurations used the used datasets.

Dataset	Model	Hidden Dim.	Layers	Learning Rate	Weight Decay	Epochs	Dropout
Tolokers2	GATv2	256	3	0.0003	0.0000	1000	0.1
Citeseer	GCN	20	2	0.0100	0.0005	200	0.0
Cora	GCN	20	2	0.0100	0.0005	500	0.0
Artnetviews	GCN	512	3	0.0003	0.0000	1000	0.1
Chameleon	GATv2	512	3	0.0003	0.0000	250	0.3
QM9	GCN	128	4	0.0010	0.0000	500	0.1
PEMS	GCN	100	3	0.0100	0.0005	500	0.0

The parameters for Section 3, GCN and GCN DE follow Table 2. The Bayesian GCN was trained using SVI [6, 21, 31, 32, 49] with a Normal surrogate distribution. The prior was initialised with standard Glorot initialization [20] scaled by 177.7. The hidden dimension was reduced to 50 to speed convergence. The Matérn GP followed Borovitskiy [7].

B Dataset Shift

Besides general uncertainty quantification in in-distribution (ID) settings, uncertainty quantification is popular in out-of-distribution (OOD) settings [38]. Like in ID settings it is important that a model can signal if it is uncertain about the prediction it makes. However, in OOD settings, the model is acting on data that is likely no longer supported by the training distribution. Thus evaluating uncertainty quantification in OOD scenarios is also very important since we expect cases where uncertainty increases to appear more often than in ID. To extend our findings to OOD we selected two datasets, one for classification (Tolokers2) and one for regression (Artnetviews), and split them into OOD and ID. Since all results held across datasets for ID, we selected the two largest datasets as representatives of the others.

To evaluate model robustness under distribution shift, we adopt the density-based split proposed by Bazhenov et al. [4]. This method partitions data based on local graph topology rather than feature distribution. However, it still introduces meaningful partitions in graph datasets, often being able to replicate splits based on features [4].

Importantly, the number of training, validation, and test examples is kept identical to the original fully ID split. We first rank all nodes by their local clustering coefficient in descending order. The first N_{test} examples, where N_{test} is the number of test examples in ID, are assigned for test, followed by N_{val} nodes for validation and N_{train} nodes for training. Consequently, test nodes correspond to those with the highest local clustering coefficients, while training nodes have the lowest. This split based on the connectedness of a node’s neighbourhood assigns denser neighbourhoods, the ones that can capture richer information, almost exclusively to the test set.

As expected, the performance in point estimation drops between ID in OOD. Specifically, for a five model ensemble for Artnetviews we register a drop in R^2 from 0.599 ± 0.003 to 0.360 ± 0.012 and

for Tolokers2 a drop in average precision from 0.617 ± 0.003 to 0.474 ± 0.007^4 . However, like the ID case, deep ensembles provide little gains over a single model for uncertainty quantification. Figure 6 shows that the gains of an ensemble for Tolokers2 are $< 1\%$ and for Artnetviews $< 3\%$ —an even worse performance than ID for Artnetviews.

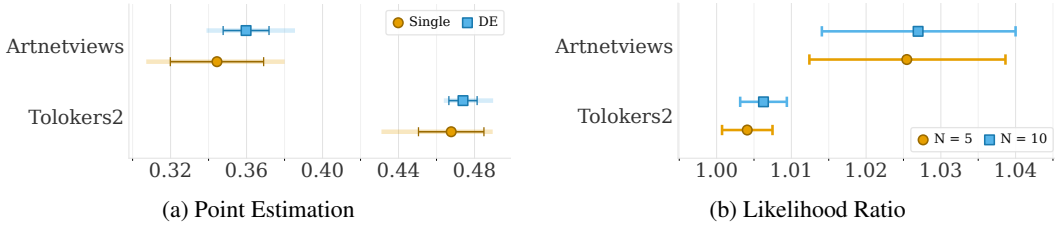


Figure 6: Comparison of point estimation performance, R^2 , for Artnetviews and average precision for Tolokers2, between an DE (5 models) and a single model. For both metrics higher score is better (a). Likelihood ratio $\exp(\text{NLL}_{\text{GNN}} - \text{NLL}_{\text{DE}})$ and 95% CI assuming normally distributed errors, quantifying the relative predictive likelihood improvement of the DE (5 models) over a single model in structural OOD shift (b).

C Other plots

Convexity. Following Section 6 we present the results of the model soup for classification in Figure 7. Like the results for regression, model soup deteriorates performance for both point prediction and uncertainty quantification. Despite the inherent limitations of accuracy, for example, the insensitivity to confidence and the threshold rigidity even the best model soup cannot reach the worst single model. Furthermore, the gaps in NLL are more pronounced than those observed for accuracy, indicating that model soup performs particularly poorly in terms of uncertainty estimation. In conclusion, even if model soup consistently matched the performance of a single model, this would still be insufficient evidence for weight-space convexity. To support that hypothesis, model soup would need to clearly outperform the single model and at least match ensemble performance [51]. The closer the gap from the model soup to the ensemble performance the stronger the weight-space convexity hypothesis holds (assuming standard optimization procedures without perfect convergence to the global optimum). In our results, model soup fails to match even the single-model baseline. Thus we argue against weight-space convexity.

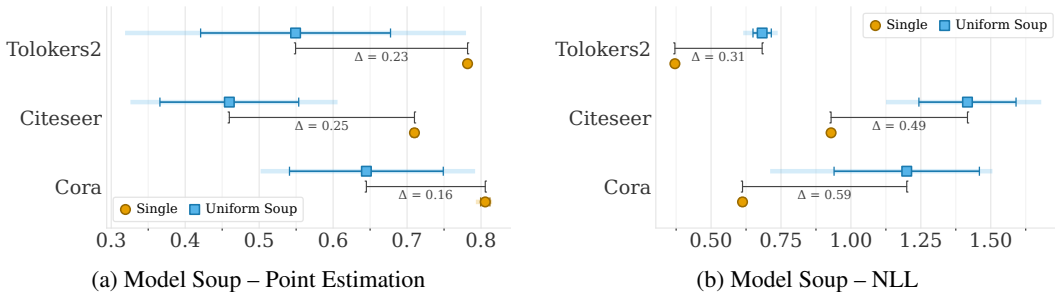


Figure 7: Weight-space convexity analysis. Figure 7a compares the point prediction performance and Figure 7b the NLL of a single model against a “model soup” formed by averaging the weights of the ensemble members. Lower values are better for NLL and higher are better for point prediction. The degraded performance of the model soup confirms that the models reside in different regions of a highly non-convex parameter space.

Dynamics. Figure 9 and Figure 8 show the dynamics of the point estimation metric and NLL for an increasing ensemble size⁵. For Artnetviews and Tolokers2 we revert back to the original metrics

⁴We use R^2 and average precision to enable easy comparison with the original work by Bazhenov et al. [5] if necessary.

⁵All experiments were performed using a NVIDIA RTX 5090 or equivalent.

used in Bazhenov et al. [5]. This should allow one to more easily compare results if necessary. Generally, the dynamics hold when changing metrics. An added bonus is that average precision, compared with accuracy, makes the dynamics easier to see.

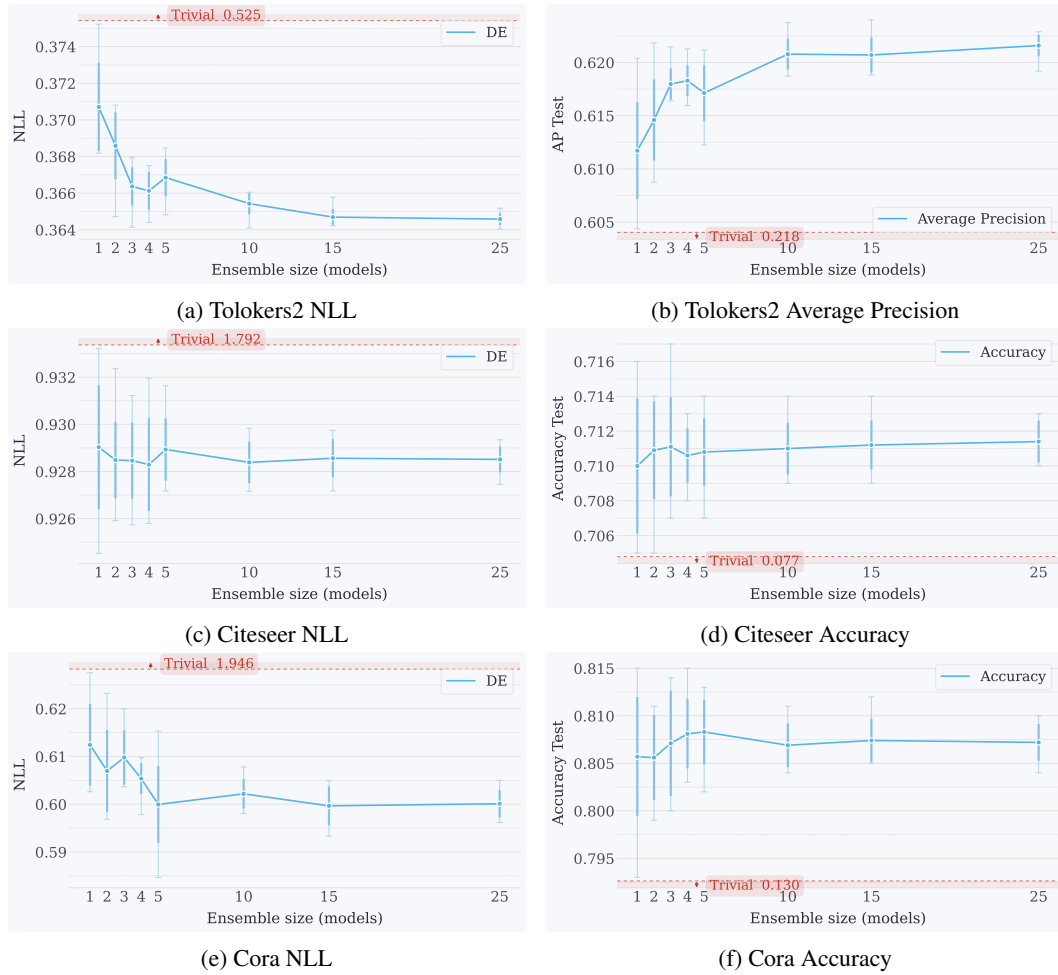


Figure 8: Evolution of NLL (a, c and e) and point estimation metric (b, d and f) as the number of base models in the ensemble increases. Red dashed line denotes a trivial baseline.

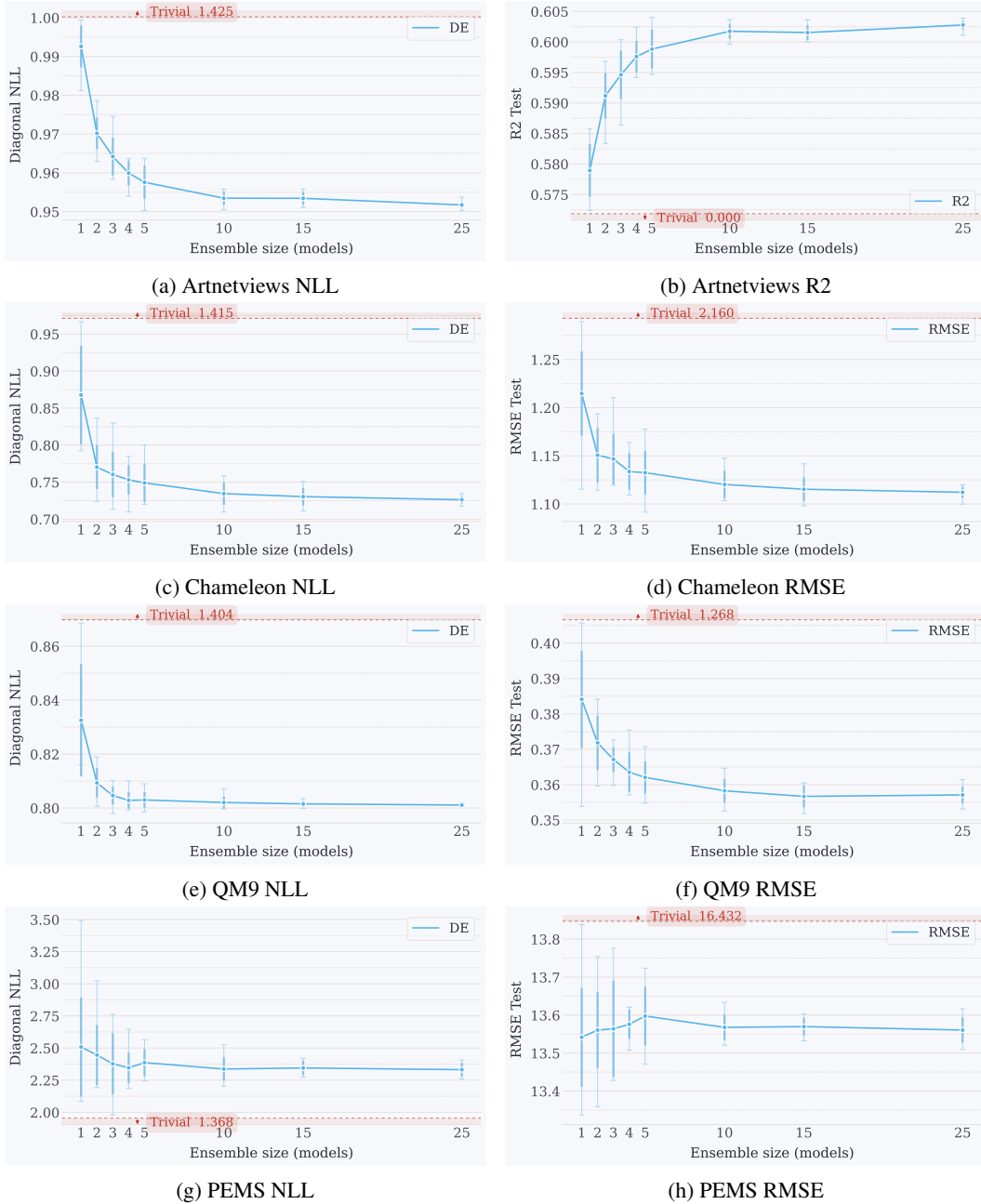


Figure 9: Evolution of NLL (a, c, e and g) and point estimation metric (b, d, f and h) as the number of base models in the ensemble increases. Red dashed line denotes a trivial baseline.